Journal of Materials Chemistry B

Accepted Manuscript

ROYAL SOCIETY OF CHEMISTRY

www.rsc.org/materialsB

Journal Name

ARTICLE

Effet of direct loading of phytoestrogens into calcium phosphate scaffold on osteoporotic bone tissue regeneration

Received 00th January 20xx,
Accepted 00th January 20xx

DOI: 10.1039/x0xx00000x

www.rsc.org/

G.Tripathi[a], R. Naren[a,b], and H.S.Yun[a*]

3D porous calcium deficient hydroxyapatite (CDHA) scaffolds with phytoestrogens were fabricated for osteoporotic bone tissue regeneration through a combination of 3D printing techniques and cement chemistry as a room temperature process. Quercetin, one of the major phytoestrogens isolated from onions and apples, was directly incorporated into CDHA for local administration in place of bisphosphonates (BPs) (which are recognized as standard treatment in osteoporosis), to avoid drug side effects. The CDHA scaffolds with quercetin (QC-CDHA) showed favorable mechanical properties (compressive strength < 21 MPa) as well as pore morphology. Quercetin was steadily released with the biodegradation of CDHA scaffolds in vitro without any initial burst. The QC-CDHA scaffolds greatly influenced both osteoblast and osteoclast cell activities. The QC-CDHA scaffolds significantly increased pre-osteoblast cell (MC3T3-E1) proliferation, differentiation, and mineralization, whereas osteoclast cell (RANK treated RAW 264.7) proliferation and differentiation were dramatically suppressed. The influence of quercetin on bone tissue regeneration was superior to alendronate, which is one of the most commonly administered BPs. All results indicated that quercetin in CDHA scaffolds plays an important role in both enhancing bone formation and suppressing bone resorption. Consequently, this technology promises great potential in osteoporotic bone tissue regeneration.

Introduction

Bone is regenerated by continuous bone resorption and bone formation throughout life. An unbalanced rate between the bone resorption process and bone formation causes a disorder of the skeletal system. Osteoporosis is a systemic skeletal disease characterized by low bone mass and bone quality due to more rapid bone resorption than bone formation, resulting in a high risk of fractures in accidents and trauma.[1] The best way to prevent bone fractures caused by osteoporosis is controlling bone metabolism by nutritional or pharmacological treatment to enhance bone quality.[2] Vitamin D and phytochemicals such as quercetin, genistein, and curcumin are nutrients that are often used as prophylactic drugs via oral administration.[3] Bisphosphonates, calcitonin, and estrogen are currently used as therapeutic agents for osteoporosis; these substances inhibit osteoclast activity and hence bone resorption, they are available by oral or local administration.[4] However, once fractures occur, bone scaffolds based in tissue engineering are often required to induce bone tissue regeneration. A high incidence of implant failure for these scaffolds is reported because of the lower regeneration capacity of osteoporotic bones compared with that of normal bone.[5] Customized scaffold designs for osteoporotic bone tissue regeneration with a function of controlling bone metabolism are consequently necessary.[6] To achieve this purpose, various metal ions such as Sr, Zn, Mg, Si, Ti, and Co have been incorporated into bone scaffolds to control osteoblast and/or osteoclast activity.[7-14] However, bioavailability and negative effects depending on each ion concentration are often considered drawbacks. Therapeutic agents or osteoprogenitor cells were also considered as functional materials to improve scaffolds effect on osteogenesis, but high cost performance, unstable state, and complicated processes all remained as weaknesses.[15] There are various reports concerning the incorporation or coating of bisphosphonates (BPs) into or on bone scaffolds. BPs such as alendronate, zoledronate, pamidronate, and risedronate are widely recognized as standard treatments for osteoporosis by inhibiting osteoclast activity at the sites of active remodeling.[16] However, BPs may contribute to side effects such as osteonecrosis of the jaw or a typical femoral fracture.[17] Furthermore, there are clear limitations to using therapeutic agents as drugs in combination with bioceramic-based scaffolds, because ceramic processes are always accompanied by sintering at high temperature and the drugs are easily denatured by heat.[18] Drugs can only be adsorbed on the surface of ceramic scaffolds after the sintering process,[19] which leads to some shortcomings, including limited

[a] Powder & Ceramic Division, Korea Institute of Materials Science (KIMS), 797 Changwondero, Changwon 641-831, Republic of Korea.
[b] Korea Universigy of Science and Technology (UST), 217 Gajeong-ro, Yeseong-gu, Daejeon, 305-350, Republic of Korea
* Corresponding author: yuni@kims.re.kr.
Electronic Supplementary Information (ESI) available: [details of any supplementary information available should be included here]. See DOI: 10.1039/x0xx00000x

adsorbable drug amount, initial burst, and rapid release of drugs.

To overcome the limitation of previous studies, we first tried to develop bioceramic scaffolds customized for osteoporotic bone regeneration by a combination of phytochemicals and our original room temperature fabrication process for ceramic scaffolds. Phytochemicals were considered as potential osteogenic drugs in place of bisphosphonates to minimize adverse effects. Phytochemicals, especially phytoestrogen molecules such as genistein, quercetin, and curcumine, are responsible for biological functions, including osteogenic, anti-osteoclastogenic, and anti-adipogenic effects [20-22]. They are typically used as nutrients to prevent osteoporosis by oral administration.[23] It has been shown that they enhance osteoblast differentiation and bone formation and the conditioned medium of estrogen-treated osteoblast cultures inhibits osteoclast development.[24] The effects of phytoestrogens on osteoblast differentiation using MC3T3-E1 cells, a mouse calvaria osteoblast-like cell line with increased alkaline phosphate activity and enhanced bone mineralization, have been previously reported.[25] However, there is no report concerning the effectiveness of phytoestrogens released from bone scaffolds to induce bone tissue regeneration. We considered the potential of quercetin, which is mainly derived from onions, apples, and grapes, as an osteogenic drug and tried direct incorporation of quercetin into the calcium phosphate scaffold through our original room temperature ceramic fabrication process.[18,26] The cement reaction of calcium phosphates was applied instead of the sintering process. 3D porous structures of ceramic scaffolds were managed by paste extruding deposition (PED) systems, which is a 3D printing technology.

α-Tricalcium phosphate (α-TCP) was chosen as a starting material to induce calcium deficient hydroxyapatite (CDHA) after cementation and was directly mixed with quercetin before fabricating 3D porous bone scaffold using the PED process. The 3D printing technology, which can produce customized and predefined pore structure and outer shape with high reproducibility using a computer-aided system, was applied to obtain ideal scaffold structure.[27] The availability of our development was carefully considered in this study. In vitro tests were carried out for both osteoblastic and osteoclastic activity by comparing CDHA scaffolds with and without quercetin from various views. The CDHA scaffolds with an optimal concentration of quercetin simultaneously promoted enhancement of bone formation and suppression of bone resorption with good mechanical properties and sustained drug release performance for extended periods of time.

Results

Fabrication of QC-CDHA scaffold

The scaffold fabrication strategy is illustrated in Scheme 1. A certain amount of quercetin was directly mixed into α-TCP

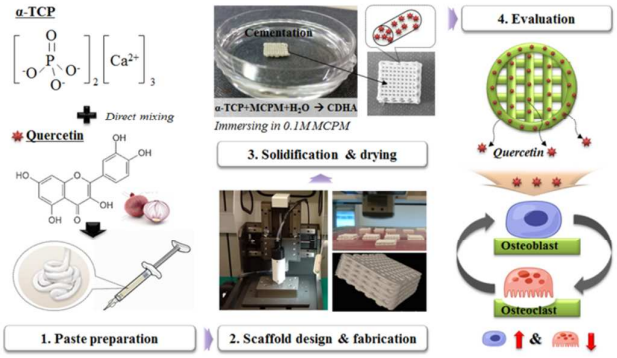

Scheme 1. Schematic diagrams and concept of the phytoestrogen loaded calcium phosphate 3D porous scaffold using a new process without sintering (MCPM: Mono calcium phosphate mono hydrate)

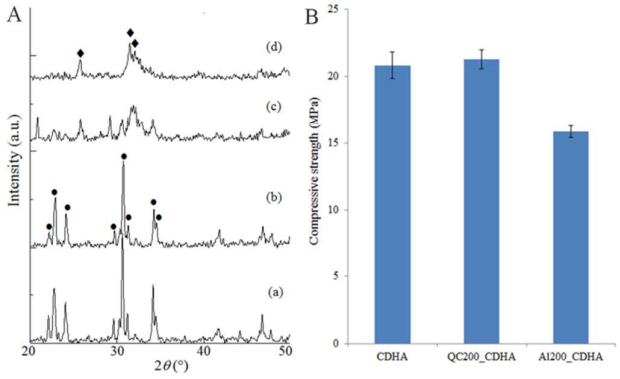

Fig.1. XRD (A) results of α-TCP powder (a), as-printed scaffold before cementation (b), after immersing scaffold in 0.1 M MCPM (c), and after immersing scaffold in DI water (d) and a comparison of the compressive strength of CDHA scaffolds with and without drugs (200 μM of quercetin and alendronate). (●: α-TCP; ♦: calcium deficient hydroxyl apatite, CDHA)

paste, which satisfies fluidity, stability, and workability to print and stack up 3D structures without deformation during 3D printing fabrication using a PED system. The α-TCP scaffold green body with controlled architectures and pore conditions under computer control was successfully fabricated as shown in Scheme 1 and was then immersed into 0.1 M of MCPM solution to solidify through the cement reaction. The XRD results of the scaffold green body were equivalent to those of α-TCP powder (Fig. 1A(a-b)). The XRD pattern showed a dramatic change in the crystal structure of the CaP after cementation from α-TCP to CDHA (Fig. 1A(c-d)). The scaffold showed mixed crystal states with α-TCP and CDHA after immersion in the 0.1 M MCPM solution for 6 h (Fig. 1A(c)). The scaffold was finally turned into CDHA when it completed cementation after immersion in DI water for three more days (Fig. 1A(d)). The addition of quercetin into α-TCP did not have an effect on the cement reaction and on the phase transformation to CDHA. The mechanical properties of α-TCP scaffold green body (before cementation) could not be evaluated because these scaffold green bodies became very soft and misshapen during the test. Meanwhile, it is noteworthy that the CDHA scaffold, which finished cementation, exhibited great mechanical properties for use as

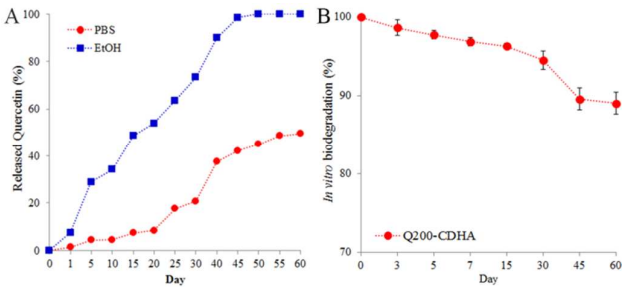

Fig.2. A: Cumulative release of quercetin loaded into CDHA by immersion in two different solvent conditions (ethanol [square] and PBS [circle]). The release kinetics was expressed in terms of release percentage based on quercetin loading amount. B: Evaluation of in vitro degradation of the CDHA scaffold for 60 days. The percentage of the remaining weight was calculated by normalizing to the weight at day 0

a bone scaffold without any further sintering process. The CDHA scaffolds showed a compressive strength of 13.8±1.3 MPa after finishing the cement reaction in 0.1 M MCPM solution and their strength increased up to 20±1.8 MPa after treatment in DI water for three days to eliminate unreacted sites and to complete the cement reaction (Fig. 1B). The compressive strength was similar to that of human cancellous bone, although the CDHA scaffolds were prepared at room temperature. The addition of quercetin into scaffolds did not have an effect on the scaffolds' mechanical properties. The QC_{200}-CDHA scaffolds exhibited a compressive strength of 21.3±0.7 MPa. Meanwhile, the addition of alendronate into scaffolds induced decreased mechanical properties; the compressive strength of Al_{200}-CDHA was 15.6±0.4 MPa. The apparent porosity of both CDHA and Q_{200}-CDHA scaffolds measured by Archimedes concept was 58.6±1 % and 62±1 %.

***In vitro* drug release and degradation of scaffold**

Quercetin is practically insoluble in water and is soluble in ethanol.[28] The drug release profile from the CDHA scaffold has been consequently evaluated both in ethanol and PBS for 60 days, as shown in Fig. 2A. Any initial burst of quercetin from the CDHA scaffold was detected under both ethanol and PBS. The quercetin from QC_{200}-CDHA in ethanol had a sustained released over time and was completely released at day 50. The release rate until day five in ethanol was rather fast (5.7 µM/day) but eventually became more constant (3.2µM/day). The release amount of quercetin from QC_{200}-CDHA in PBS was much less than the release observed in ethanol due to the solubility difference. Only 50% (by weight) of the quercetin consistently released from the scaffold within the entire test period (60 days). In contrast to the release profile in ethanol, the release rate for the initial period until day 20 was lower (0.85µM/day) than the later time period. It appears that the driving force of quercetin release under PBS is related to physical conditions with degradation of the CDHA scaffold because quercetin is not soluble in aqueous conditions. The in vitro biodegradation of the QC-CDHA scaffold was tested under PBS at 37^{0}C for 60 days (Fig. 2B). The release profile of

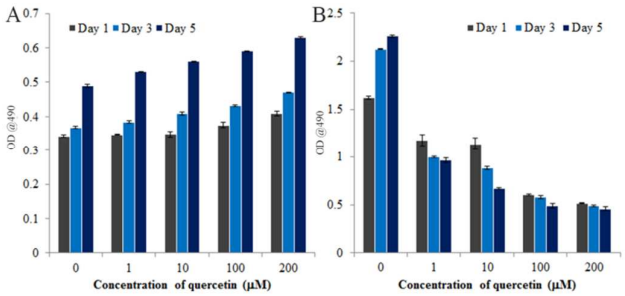

Fig.3. Effect of different quercetin amounts (0–200µM) on proliferation of both MC3T3-E1 cells (osteoblast) (A) and RAW 264.7 cells with RANKL (osteoclast) (B) at 1, 3, 5 days of culturing (n = 4 samples per group)

quercetin was similar to the degradation profile in PBS. QC_{200}-CDHA scaffolds slowly decreased in weight during the initial period and the degradation amount was slightly increased during the later time period. A total degradation of 11% (by weight) was detected over 60 days.

***In vitro* cell proliferation**

Both osteoblasts (MC3T3-E1) and osteoclasts (RANKL treated RAW 264.7) were cultured with different concentrations of quercetin (0, 10, 100, 200 µM) for different time intervals (1, 3, 5 day) to test drug efficiency on the proliferation of both cells and to determine the most effective drug concentration (Fig. 3). The osteoblast cell numbers were gradually increased with time and showed the highest cell proliferation at day 7 (Fig. 3A). Quercetin was shown to enhance osteoblast cell proliferation; higher concentrations of quercetin resulted in higher cell proliferation efficiency for each time period, with 200 µM of quercetin exhibiting the highest cell proliferation. Alternatively, the proliferation of osteoclast cells without quercetin also gradually increased with time and showed the highest cell proliferation at day 7 (Fig. 3B). However, osteoclast cell proliferation was dramatically suppressed by the addition of quercetin and resulted in decreased cell numbers for each culturing time. Higher concentrations of quercetin significantly suppressed osteoclast cell proliferation, with 200µM quercetin showing the lowest cell proliferation. Therefore, quercetin simultaneously promoted osteoblast proliferation and suppressed osteoclast proliferation. The effects of quercetin were much more dramatic than alendronate, which is well known as a standard treatment for osteoporosis under the same concentrations (supporting information1; SI-1). Alendronate did not have an effect on osteoblast proliferation; it exhibited a suppression of osteoclast cells but the effects of quercetin were far greater.

Quercetin was directly mixed with α-TCP paste in this study and contained in CDHA scaffolds. The effect of the quercetin that was released from CDHA scaffold was studied for both osteoclasts and osteoblasts. Both cells were seeded on CDHA, QC_1-CDHA, and QC_{200}-CDHA scaffolds, cultured for 1, 3, and 5 days, and analyzed by calorimetric MTS assays (Fig. 4). The quercetin in CDHA scaffolds was still effective in cell activities similar with direct loading. The QC_{200}-CDHA scaffold exhibited

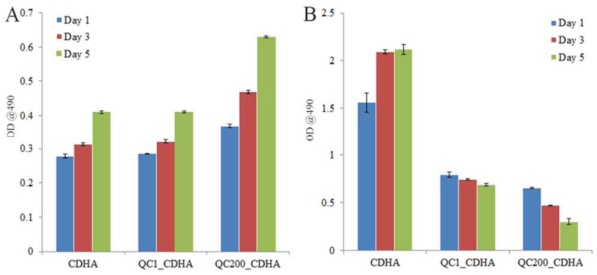

Fig.4. Comparison of MC3T3-E1 (osteoblast) (A) and RAW 264.7 with RANKL (osteoclast) (B) cell proliferation at 1, 3, 5 days of culturing on CDHA scaffolds, QC_1-CDHA scaffolds, and QC_{200}-CDHA scaffolds (n = 4 samples per group)

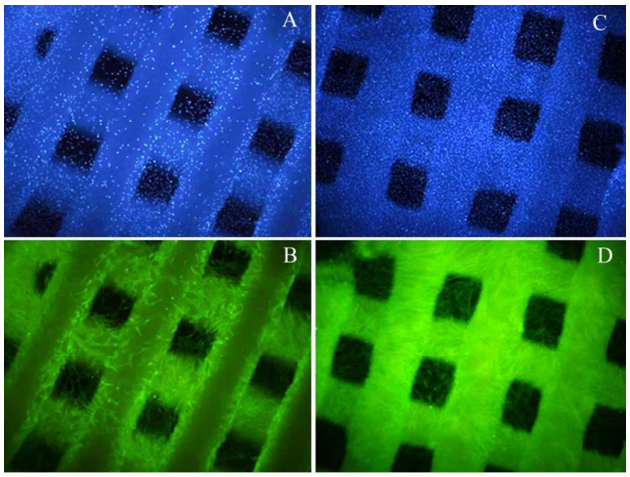

Fig.5. Top-view fluorescence microscope images (X4) of CDHA scaffolds (A, B) and QC_{200}-CDHA scaffolds (C, D) after five days of MC3T3-E1 osteoblast cell culturing

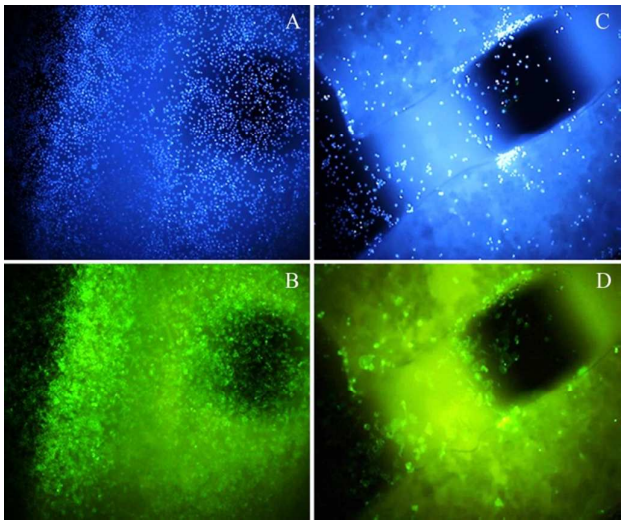

Fig.6. Top-view fluorescence microscope images (X10) of CDHA scaffolds (A, B) and QC_{200}-CDHA scaffolds (C, D) after five days of RAW 264.7 with RANKL cell culturing

much enhanced osteoblast proliferation at day 5 compared with CDHA scaffolds (Fig. 4A). Meanwhile, the QC_{200}-CDHA provided a dramatic suppression of osteoclast proliferation (Fig. 4B). Both QC_1-CDHA and QC_{200}-CDHA showed a large

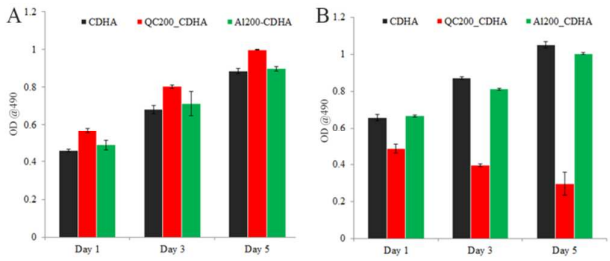

Fig.7. Comparison of MC3T3-E1 (osteoblast) (A) and RAW 264.7 with RANKL (osteoclast) (B) cell proliferation at 1, 3, 5 days of culturing on CDHA scaffolds, QC_{200}-CDHA scaffolds, and AL_{200}-CDHA scaffolds (n = 4 samples per group)

reduction in cell number and cell proliferation with time. Higher concentrations of quercetin (QC_{200}-CDHA) showed a higher suppression effect on osteoclast proliferation. Similar results may also be confirmed by fluorescent microscope images (Fig. 5, Fig 6, and SI 2-3). 3D printed CDHA scaffolds exhibited good cell affinity. Osteoblast cells were flattened, polygonal shaped, and well spread, with highly extended and numerous filopodia, as shown in Fig. 5 and SI 2. It can be observed that the cells migrate well through 3D scaffold structures and are capable of creating a dense network. A significant difference in cell numbers were observed between the CDHA and QC_{200}-CDHA scaffolds as we may expect based on MTS results. MC3T3-E1 cells on the QC_{200}-CDHA scaffold showed superior cell numbers as compared with the CDHA scaffold and also formed a much denser cell network because of quercetin's effect. In contrast to osteoblasts, osteoclast cells showed different behavior on CDHA and QC_{200}-CDHA scaffolds (Fig. 6). RANKL treated RAW 264.7 cells on CDHA without quercetin were well proliferated with a high cell number and formed a dense cell network throughout the 3D scaffold's structure. Conversely, the osteoclast cell number was extremely decreased on the QC_{200}-CDHA scaffold because quercetin suppresses osteoclast cell activity. The effect of alrendronate loaded into CDHA scaffolds (Al_{200}-CDHA) did not show such dramatic effects as QC_{200}-CDHA for both cells' proliferation (Fig. 7 and SI 4). Al_{200}-CDHA slightly suppressed osteoclast cell proliferation, whereas no change was observed for osteoblast cell proliferation.

In vitro cell differentiation

The differentiation of osteoblast cells cultured on CDHA scaffolds with and without quercetin was assessed in terms of the ALP activity of MC3T3-E1 cells after 7, 14, and 21 days (Fig. 8A). The ALP activity was significantly increased in both CDHA and QC_{200}-CDHA scaffolds with increased incubation time. The increased ALP activity in cells may indicate that CDHA still supports the bone forming potential of cells on their surfaces at late incubation time periods. The ALP activity of osteoblasts on the QC_{200}-CDHA scaffolds was higher than on the CDHA scaffolds, indicating significant up-regulated osteoblastic differentiation of the cells on the QC_{200}-CDHA scaffold due to the effect of quercetin.

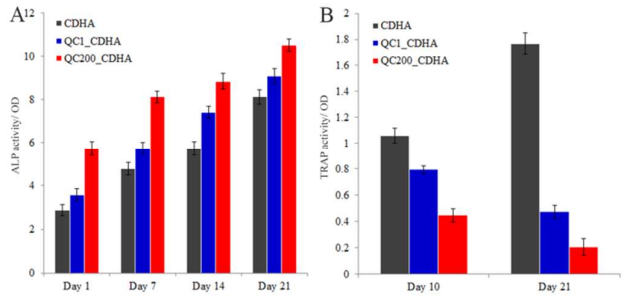

Fig.8. ALP activity of MC3T3-E1 cells (A) and TRAP activity of RAW 264.7 cells with RANKL (B) on three types of scaffolds. Data are presented as the mean ± SD (n = 4 samples per group). (Fig. 9E)

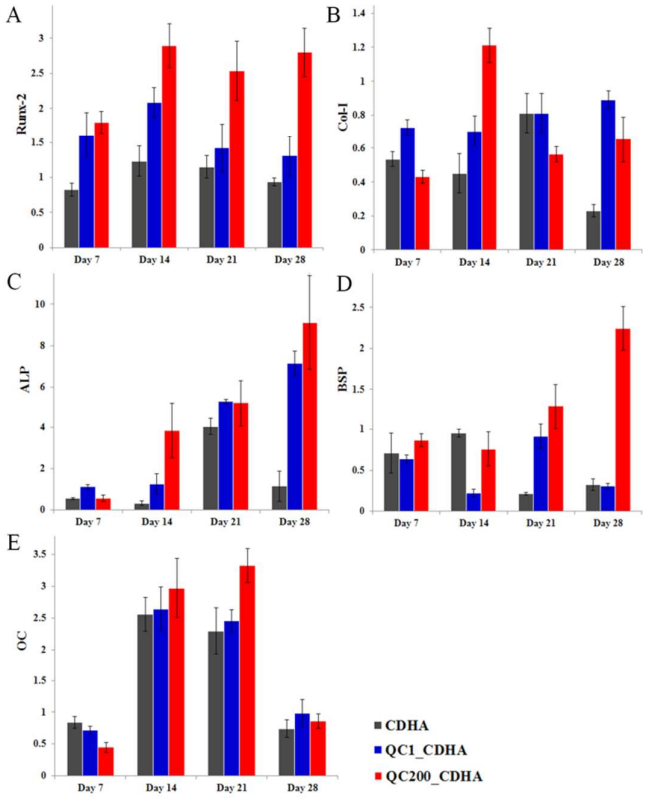

Fig.9. Quantitative real-time PCR analysis of RUNX-2 (A), Col-I (B), ALP (C), BSP (D), and OC (E) m-RNA expression in cells grown on each scaffold at 7, 14, 21, 28 days of culturing. Data are presented as the mean ± SD (at least n = 4 samples per group)

Similar results were obtained from the real-time PCR analysis. Key osteoblast genes, such as RUNX-2, Col-I, ALP, BSP, and OC, were selected to evaluate the effect of the differentiation process at the mRNA level (Fig. 9). RUNX-2 is the master gene in osteogenesis and is the key transcription factor regulating osteoblast differentiation.[29] The expression of RUNX-2 in all samples increased until day 14 and no more increases were observed after day 14 (Fig. 9A). The QC_{200}-CDHA scaffold expressed the highest level of RUNX-2 at day 14. Col-I is regularly used as an early marker of osteoblast differentiation.[30] The level of Col-I in the QC_{200}-CDHA scaffold was also the highest at day 14 but down-regulated from day 21 when differentiation started (Fig. 9B). ALP is known as one of the main intermediate osteogenic differentiation makers preparing the extracellular matrix (ECM) for the subsequent mineralization stage.[31] ALP expression in cells grown on QC_{200}-CDHA exhibited a dramatic increase at day 14, whereas ALP expression on both CDHA and QC_1-CDHA scaffolds significantly increased at day 21 (Fig. 9C). Therefore, the QC_{200}-CDHA scaffold initiated a more rapid differentiation of osteoblasts than the other scaffolds. BSP is a phosphorylated non-collagenous protein expressed only in mineralized tissues such as newly formed bone and cementum.[32] It is an important regulator for bone mineralization by binding to the HA crystals, therefore triggering HA nucleation. BSP gene expressions by MC3T3-E1 cells were generally increased on HA-containing scaffolds up to four weeks. BSP gene expression on the QC_{200}-CDHA scaffolds was highest and increased with time until day 28 (Fig. 9D). The elevated expression of BSP on the QC_{200}-CDHA scaffold suggests a higher mineralized matrix on the QC_{200}-CDHA scaffold. OC is secreted by osteoblasts and plays a role in mineralization and calcium homeostasis. Consequently, it is often used as a terminal marker of osteoblast differentiation.[33] The highest level of OC was observed in the QC_{200}-CDHA scaffold at day 21 (Fig. 9E). The early increased expression of OC in cells grown on QC_{200}-CDHA may be due to the fact that mineralization occurred much sooner based on quercetin's effect. That is, the presence of quercetin may have been a key factor promoting stimulation of the osteogenic differentiation of osteoblast cells.

The effect of quercetin on the differentiation of osteoclast cells was studied by evaluating TRAP activity (Fig 8B). TRAP activity is regarded as an important cytochemical marker of osteoclasts; its concentration in serum is utilized as a biochemical marker of osteoclast function and the degree of bone resorption.[34] Expression of TRAP is associated with the activation and differentiation of osteoclasts. Osteoclast differentiation of RAW 264.7 cells was induced by treating RANKL (200 ng/ml) for 10 and 21 days on CDHA, QC_1-CDHA, and QC_{200}-CDHA scaffolds. TRAP activity of osteoclasts decreased with higher concentrations of quercetin. Furthermore, TRAP activity of cells on QC-CDHA scaffolds with 1 and 200 μM of quercetin decreased with culturing time, whereas TRAP activity on CDHA without quercetin significantly increased with culturing time. These results prove that quercetin loaded in CDHA ceramic scaffolds is effective on the suppression of osteoclast differentiation in parallel with the activation of osteoblast differentiation.

In vitro cell mineralization

Calcium mineralization was determined by alizarin red-S (ARS) staining of MC3T3-E1 cells at 14 and 21 days. ARS is an early stage marker of matrix mineralization and its appearance is an important step towards the formation of the calcified extracellular matrix associated with bone.[35] The scaffolds will be stained red when immersed in alizarin, if it contains calcium due to the mineralization. The QC_{200}-CDHA scaffold exhibited a much thicker (dark) red colour than the CDHA scaffold (Fig. 10A and SI-5). A quantitative evaluation of ARS expression was

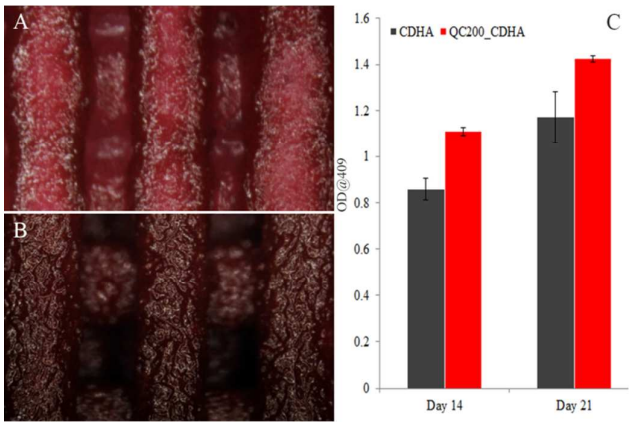

Fig.10. Alizarin red S staining images of CDHA (A) and QC_{200}-CDHA scaffolds after day 14, and comparison of expression values after 14 and 21 days of culturing. Data are presented as the mean ± SD (n = 4).

also studied and showed that the CDHA scaffold containing quercetin induced a significant increase in the mineralization rate of osteoblast cells (Fig. 10B).

Discussions

In this study, quercetin, which is one of the major phytoestrogens isolated from onions, apples, and grapes, was first incorporated into bioceramic scaffolds as local administration to enhance the function of the scaffolds in osteoporotic bone tissue regeneration. Osteoporosis commonly causes imbalance between bone forming osteoblasts and bone resorbing osteoclasts, generally resulting from estrogen deficiency. A common treatment for osteoporosis is using an anabolic agent that stimulates bone formation and anti-resorptive agents including BPs and estrogen that inhibit osteoclast differentiation and activity. Phytoestrogens are plant-derived nonsteroidal compounds that bind to estrogen receptors and have estrogen-like activity.[36] Phytoestrogens are commonly used as nutritional supplements because of their potential beneficial role in the prevention and treatment of cardiovascular diseases and osteoporosis. Phytoestrogens have recently been considered as osteogenic drugs in place of the typical anti-resorptive agents such as alrendronate and zolendronate, to minimize adverse effects. Wong et al. used a collagen matrix to graft quercetin into bony defects and reported the potential possibility of quercetin as a local bone induction agent.[37] We have investigated the efficiency of quercetin on bone regeneration and sought to achieve an ideal scaffold for osteoporotic bone tissue regeneration through the combination of quercetin and our original process of constructing a bioceramic scaffold at room temperature using 3D printing techniques.

To date, it has only been possible to incorporate biologically active molecules and drugs into ceramic scaffolds for bio-functionalization by adsorption after a sintering, because ceramic processes must include sintering to remove their binder and to obtain stabilized mechanical properties. However, most bioactive molecules are easily denatured by the heat. This conventional process results in a very limited incorporation of bioactive molecules and an unstable state, which leads to large initial burst amounts and short release periods. We introduced a novel strategy whereby quercetin was directly blended with α-TCP to prepare an extruding paste for the PED system. We were able to extrude this paste continuously and homogeneously during the PED process, which consequently allowed us to design and fabricate 3D porous scaffolds with various morphologies and pore structures under computer control because cement reaction was not induced yet at this stage. The required structural condition of scaffold in tissue engineering could be cleared through this step. The α-TCP scaffold green body was then hardened and stabilized by phase transformation to CDHA by immersing the α-TCP scaffold green body in 0.1 M MCPM solution and DI water.[38] Quercetin did not release from the scaffold during this process because of its insolubility in aqueous solutions. Suitable mechanical properties to match those of the tissue at the site of implantation are also required for scaffolds. Adequate mechanical properties for bone tissue regeneration were obtained; the compressive strength of the CDHA scaffold was as high as 20±1.8 MPa whereas that of cancellous bone is 0.1~16 MPa. The addition of quercetin did not have an effect on mechanical property regardless of the concentration. Meanwhile, the effect of alendronate on both setting time and the mechanical properties of calcium phosphate bone cement was reported by Zhao et al.[39] The addition of alendronate into α-TCP consequently initiated a 25% reduction in the mechanical properties of the CDHA scaffold because our process also applied a calcium phosphate cement reaction during solidification.

Quercetin should be homogeneously distributed throughout the scaffold because quercetin was directly mixed with α-TCP powder before 3D structure fabrication. If quercetin is located only in the surface of the scaffold by a conventional coating process, it will be rapidly released in a short period of time when immersed in ethanol because quercetin exhibits a high solubility in ethanol. However, the quercetin in our scaffolds was constantly released over time for 50 days without any initial burst in ethanol, which proved that quercetin was homogeneously distributed. Furthermore, quercetin was released very slowly in PBS with degradation of the scaffold over time, because quercetin shows very low solubility in aqueous conditions. Therefore, the release rate of quercetin may be controlled by adjusting the biodegradability of the scaffold. These results suggest that QC-CDHA scaffolds have a potential use as a drug delivery matrix for the long-term local administration of quercetin to treat osteoporosis.

Osteoporosis can affect both osteoblast and osteoclast activity. To achieve high efficiency for scaffolds in osteoporotic

bone tissue regeneration, osteoblastic cell activity should be enhanced, while osteoclastic cell activity should be suppressed. The concentration of quercetin had a significant effect on both cell activities. Higher concentrations of quercetin exhibited increased regulation of both cell types. There were no adverse effects with increasing concentrations of quercetin. That is, 200μM of quercetin dramatically increased osteoblast proliferation (141% enhancement) at day 5 compared with the CDHA scaffold without added quercetin. This concentration of quercetin also simultaneously suppressed osteoclast proliferation (83% reduction). Meanwhile, 200μM of alendronate only affected osteoclast proliferation, with a 104% increase of osteoblast proliferation and a 68% decrease of osteoclast proliferation. Quercetin provides better efficiency than alendronate under the same concentration conditions of this study because alendronate is generally treated with higher concentrations than 200μM.[40]

Although quercetin is insoluble in cell culture media, quercetin incorporated into CDHA scaffolds may still affect the activity of both cells because CDHA is biodegradable and quercetin could be released from the CDHA scaffold with degradation of CaP. The QC_{200}-CDHA scaffold significantly increased osteoblast cell proliferation and decreased osteoclast cell proliferation over time as compared with the CDHA scaffold. Osteoblast cell proliferation was enhanced by 153% and osteoclast cell proliferation was suppressed by 86%. Alendronate from CDHA scaffolds also affected cell proliferation activity but only for osteoclasts. Al_{200}-CDHA suppressed osteoclast cell proliferation by 50%, which is 36% less than the suppression exhibited by the QC_{200}-CDHA scaffold.

Furthermore, the effective influence of quercetin from the CDHA scaffold on the differentiation behaviour of both cells was proved by studying ALP activity, real-time PCR gene expression, and TRAP activity. ALP activity is an established marker for the osteoblast phenotype. It is generally accepted that an increase in ALP activity in a population of bone cells reflects a shift to a more differentiated state.[41] Moreover, ALP appears to play a crucial role in the initiation of matrix mineralization. ALP activity of MC3T3-E1 cells on all types of scaffold was increased for all time periods. There was a significant difference in ALP activity between CDHA scaffolds and QC-CDHA scaffolds with an increase in the concentration of quercetin after every time period. Quercetin released from CDHA scaffold clearly accelerated the differentiation efficiency of osteoblast cells. During osteogenic differentiation, the genetic expressions of bone markers such as Col-I, RUNX-2, ALP, BSP, and OC are also up-regulated at a stage of differentiation by the addition of quercetin and studied in detail by real time-PCR. After the proliferation phase, osteoblasts differentiate and produce the extracellular matrix. RUNX-2 is a transcription factor that controls skeletal development by regulating the differentiation of osteoblasts and it is essential for bone formation. RUNX-2 has a major effect on osteogenesis by stimulating the gene expression of Col-I, ALP, and OC. Col-I is the most abundant protein synthesized by active osteoblasts and it is conductive to mineral deposition. ALP is an early marker of osteoblast phenotypes and differentiation with the production of Col-I. BSP is a non-collagenous protein expressed only in mineralized tissue and is an important regulator for bone mineralization. OC is synthesized by mature osteoblasts before and during matrix mineralization. The expression of each of these genes was dramatically activated by the addition of quercetin. Both RUNX-2 and Col-I expressed maximum values at day 14 for the QC_{200}-CDHA scaffold, which proves effective initiation of early stage differentiation in comparison with the CDHA scaffold. The expression of ALP normally increases with the start of differentiation and is then down-regulated after the mineralization stage begins. The QC_{200}-CDHA scaffold showed the highest ALP expression without down-regulation over time due to continuous proliferative stimuli from phytoestrogen, which induced continuous proliferation and differentiation even after the beginning of mineralization, whereas ALP expression with the CDHA scaffold began down-regulation at day 28. Both BSP and OC, which are markers of bone mineralization, also showed the highest value with the QC_{200}-CDHA scaffold, proving the positive effect of quercetin on bone tissue regeneration as compared with the CDHA scaffold. The results of TRAP activity, which was studied to evaluate osteoclast differentiation, additionally provided clear evidence of quercetin's effect on bone metabolism. The TRAP activity of RAW 264.7 cells with RANKL on CDHA at day 21 was 167% up-regulated from day 10, indicating the differentiation of osteoclast cells. However, TRAP activity of cells on both QC_1-CDHA and QC_{200}-CDHA at day 21 was down-regulated by 40% and 54%, respectively from day 10, exhibiting suppression of osteoclast cell differentiation by quercetin. Furthermore, ARS staining results suggested that the quercetin from the CDHA scaffold promoted the enhancement of bone mineralization during bone tissue regeneration. All results of the in vitro study indicate that the presence of quercetin in CDHA scaffolds can accelerate osteoblast activity while simultaneously inhibiting osteoclast activity, consequently enhancing osteoporotic bone tissue regeneration.

Experimental

Preparation of CDHA scaffold

CDHA scaffolds were prepared through three steps, as shown in Scheme 1. The first step was the preparation of printing paste with proper rheological characteristics and formability for stacking a stable 3D structure. The α-TCP paste was prepared by mixing α-TCP powder (<25 μm) and 1% hydroxypropyl methyl cellulose (HPMC, Sigma), which was dissolved in 30% ethanol. The powder/liquid ratio was 1 to 0.5 (wt:vol). Quercetin (CAS No.:6151-25-3, Wako Laboratory Chemicals), being hydrophobic in nature, was first dissolved in ethanol, then mixed into HPMC solution, and added into α-TCP powder to prepare the quercetin-laden CDHA scaffolds. Numerous concentrations of quercetin (1–200μM) were tested against both osteoblast and osteoclast type cells to optimize the most effective concentration. Three set of scaffolds were primarily evaluated in this study: CDHA, QC_1-CDHA (1μM

concentration of quercetin in CDHA scaffold), and QC_{200}-CDHA (200μM concentration of quercetin in CDHA scaffold). The same concentration of alendronate in CDHA scaffolds (Al-CDHA) was also prepared to compare drug efficiency on both osteoblasts and osteoclasts.

The second step was the fabrication of the calcium phosphate (CaP) green scaffold without cementation with α-TCP paste using a PED system. The α-TCP paste housed in the syringe was deposited through a cylindrical nozzle of 21 gauge by our original PED system. The shapes and sizes of the scaffold could be designed at discretion and could be controlled by a computer system. A gantry robotic deposition apparatus was used, equipped with specially-altered systems including an actuator to control the position of the deposition nozzle for the fabrication of the scaffold. Three axes of motion control (x, y, and z-axis) were provided by the gantry system, and a material delivery assembly composed of a syringe as a reservoir was affixed onto the z-axis motion stage. The z-axis motion stage assembly was mounted on a moving x gantry to enable the controlled motion of the mounted syringe in three dimensions.

The final step was solidification of the scaffold through cement reaction. The α-TCP scaffold green body was dried at room temperature for one day, followed by immersion in 0.1 molar (M) monocalcium phosphates monohydrate (MCPM) solution for 6 h to induce hardening by the cement reaction in place of sintering. 3.0 ml of 0.1 M MCPM solution was optimized for setting of each scaffold. In this step, α-TCP was converted to CDHA. The CaP scaffolds were then washed with deionized (DI) water several times and dried completely at room temperature for three days prior to further experiments.

Characterization

The phase composition of α-TCP and CDHA was determined using X-ray diffraction (XRD, DMAX-2200, Rigaku) powder diffractometry (CuK α1 radiation) operating at a voltage of 36 kV. Measurements were taken at a 2θ angle range of 10–60°. The particle size of α-TCP powder was observed by a particle size analyzer (LS™13 320 MW, Beckman Coulter). The compressive strengths and moduli of scaffolds were measured using a uniaxial testing machine with a 5 kN load cell (RB Model 302 MLTM; R&B, Korea) at a crosshead speed of 1 mm/min. Five samples (10 × 10 × 4 mm) were tested against each set.

***In vitro* degradation**

The scaffolds were used to perform an in vitro degradation test in phosphate buffered saline (PBS) (pH 7.4) at 37^0C while gently agitated. For *in vitro* degradation scaffolds were immersed in PBS and the volume taken was, PBS: scaffold = 100:1 volume ratio. Samples were collected after predetermined time periods, washed in deionized water, and dried at room temperature for two days. The remaining weight of the scaffold was determined using the following equation (n = 4):

$$Remaining\ weight\ (\%) = 100 - \left[\frac{(Wi - Wd)}{Wi} * 100\right]$$

Where W_i is the initial weight of the scaffold and W_d is the dry weight of the scaffold after incubation.

Drug release profile

The drug release profile of the scaffolds was carried out as follows. Scaffolds were placed in separate test tubes (n = 4). We tested the drug release against ethanol and PBS at 37^0C. The amount of quercetin released from the scaffolds was estimated by collecting solvent from the test tubes and replacing it with an equal amount of fresh solution. The same procedure was repeated until the complete release of the drug. The concentration of the released drug was determined spectrophotometrically at 256 nm; the released quantity was calculated from the standard curve.

Pre-treatment of scaffold and cell culture

The scaffolds were sterilized by immersion in 70% ethanol for 1 h under UV and were then washed with PBS several times. The scaffolds were kept immersed overnight in cell culture media without cells at standard incubation condition to avoid any contamination or pH change during the culture process.

The MC3T3-E1 cells (Subclone 4, ATCC CRL-2593, obtained from ATCC) were selected as osteoblastic cells and were cultured in α-minimum essential medium (α-MEM) (Gibco) supplemented with fetal bovine serum (FBS, Gibco) and penicillin (Keunhwa pharmaceutical) and streptomycin (Donga pharmaceutical) under standard culture conditions at 37^0C, 5% CO_2. The receptor activator of nuclear factor kappa-B ligand (RANKL) treated RAW 264.7 cells (RAW 264.7 (ATCC® TIB-71™)) were used as osteoclastic cells and were cultured under the same conditions with the osteoblasts. When the cells reached 80% confluence, they were trypsinized, collected through centrifugation, and processed further with scaffolds.

Cell proliferation

The cell proliferation of both MC3T3-E1 and RANKL treated RAW 264.7 cells was evaluated using a colorimetric 3-(4, 5-dimethylthiazol-2-yl)-5(3-carboxymethonyphenol)-2-(4-sulfophenyl)-2H-tetrazolium (MTS) assay (CellTiter 96® AQeous One solution Cell Proliferation Assay Promega), according to the manufacturer's instructions. The cells were seeded at a density of 1.0×10^4 cells/scaffold on both CDHA and QC-CDHA scaffolds, followed by the addition of a complete growth medium after 2 h of standard incubation. The growth medium was replaced with a fresh medium routinely to eliminate non-adherent cells throughout the experiment. The MTS tetrazolium compound was bio reduced by cells into a coloured formazan product that is soluble in tissue culture medium that absorbs maximally at 490 nm. The cell proliferation was evaluated for day 1, 3, and 5.

The cell morphology and cell material contacts were studied using fluorescence microscopy. After seeding cells on the scaffolds and followed by proper incubation for the required time period, cells were fixed on samples by 4%

formaldehyde in 1XPBS for 30 min. The cells were then permeabilized by 0.1% TritonX-100 in 1XPBS. Subsequently, the cells were washed twice with 1XPBS and blocked with 1% BSA in 1XPBS. After washing the cells twice, Alexa Fluor 488 Phylloidin and DAPI (NucBlue® Fixed Cell ReadyProbes® Reagent, Life technologies) were added to stain the cytoskeleton and nucleus of the cells, respectively. This was followed by washing the cells twice with 1XPBS, prior to observation under fluorescence microscope (Olympus IX71, Olympus, Japan).

Alkaline phosphate activity

The alkaline phosphatase (ALP) activity was measured using QuantiChrom™. The ALP Assay Kit (DALP-250) was provided by BioAssay systems. Following the kit protocol, cultures were washed three times with $CaCl_2$ and $MgCl_2$ free PBS. The culture was lysed in 0.5 mL 0.2% Triton X-100 in distilled water for 20 min. The working solution was prepared with 200 µL of the assay buffer, 5 µL of Mg acetate, and 2 µL of pNPP. A 5µL volume of the supernatant was mixed with 195 µL of the working solution. The solution was immediately put into a plate reader and optical density measurements were taken at 405 nm at 0 and 4 min. ALP measurements were taken on days 1, 7, 14, and 21.

Quantitative real-time polymerase chain reaction

A quantitative real-time polymerse chain reaction (real-time PCR) was carried out using the Thermal Cycler Dice® Real Time System II (TAKARA, Japan). MC3T3-E1 cells were seeded at a density of 1.0×10^5 cells on CDHA and QC-CDHA scaffolds (n = 4). Cells were harvested at predetermined time points and total RNA was isolated using illustra RNA spin Mini RNA isolation Kit (GE Healthcare) according to the manufacturer's instructions. cDNA was synthesized using Superscript II (Invitrogen) and PCR reactions were performed with osteogenic marker primers (collagen type I [Col-I], runt-related transcription factor 2 [RUNX-2] alkaline phosphatase [ALP], bone sialoprotein [BSP) and osteocalcin [OC]) in ABI 7500 real-time PCR instrument (Applied Biosystems). Quantitative real-time PCR was carried out with the following primers: RUNX2 (s 5'-TAA GAA GAG CCA GGC AGG TG-3'; as 5'-TGG CAG GTA CGT GTG GTA GT-3'), Col-I (s 5'-ATC CAA CGA GAT CGA GCT CA-3'; as 5'-GGC CAA TGT CTA GTC CGA AT-3'), ALP (s 5'-CTT GAC TGT GGT TAC TGC TG-3'; as 5'-GAG CGT AAT CTA CCA TGG AG-3'), BSP (s 5'- GAG CAG AGA CCA CAC CCC AA-3'; as 5'- TTC CTC GTC GCT TTC CTT CA-3'), and OC (s 5'-TGC TTG TGA CGA GCT ATC AG-3'; as 5'-GTG ACA TCC ATA CTT GCA GG-3'). Each sample was analyzed in triplicate and normalized to the expression of housekeeping gene glyceraldehyde 30 phosphate dehydrogenase (GAPDH) and were expressed as fold changes relative to the expression level(the $2^{-\Delta\Delta Ct}$ method was used). Finally, real-time PCR reactions were run at 95^0C for 10 min followed by 95^0C for 5 sec, 60^0C for 30 sec, and 72^0C for 1 min for 40 cycles; the dissociation curve was completed at 95^0C for 5 sec and 60^0C for 30 sec.

Tartrate-resistant acid phosphatase (TRAP) assay

Osteoclast differentiation was tested by tartrate-resistant acid phosphatase (TRAP) assay. The scaffolds (n=4) were seeded with osteoclast type cells under standard incubation conditions. Cells were collected from scaffolds at predefined intervals and were lysed with a 1XRIPA buffer and were collected following by centrifugation at 4^0C. The supernatants were incubated with p-nitrophenyl phosphate solution for 30 min at 37^0C and the reaction was stopped by adding 500 µl of 1 N NaOH. TRAP activity was determined by measuring the conversion of p-nitrophenyl phosphate to p-nitrophenol. Optical density was determined using a microplate reader at a wavelength of 405 nm.

Alizarin red staining

Osteoblast monolayers on developed scaffolds were washed with 1XPBS and fixed in 10% (v/v) formaldehyde (Sigma–Aldrich) at room temperature for 15 min. The monolayers were then washed twice with DI water prior to the addition of 1 mL of 40 mM ARS (pH 4.1) per well followed by gentle shaking at room temperature for 20 minutes. After aspiration of the unincorporated dye with dH_2O, scaffolds were stored at -20^0C prior to dye extraction. Stained monolayers were visualized using an inverted microscope (Nikon). For the quantification, 800 µL of 10% (v/v) acetic acid was added to each well, and the plate was incubated at room temperature for 30 min by shaking. The monolayer, now loosely attached to the plate, was then scraped from the scaffold with a cell scraper (Fisher Life Sciences) and transferred with 10% (v/v) acetic acid to a 1.5 mL micro centrifuge tube, overlaid with 500 µL mineral oil (Sigma–Aldrich), heated to exactly 85^0C for 10 min, and then transferred to ice for 5 min. A part of supernatant was taken out, and 10% (v/v) ammonium hydroxide was added to neutralize the acid. Aliquots of the supernatant were read in triplicate at 405 nm in a 96-well format using opaque-walled, transparent-bottomed plates (Thermo Scientific).

Statistical analysis

The results were expressed as mean ± standard deviation. Statistical analyses were performed using GraphPad Prism (GraphPad Software Institute, CA, USA). Treatment effects were analyzed using one-way ANOVA. Significance was set at $P < 0.05$.

Conclusions

We demonstrated the possibility of using phytoestrogens as new additives in ceramic scaffolds with the function of local administration to accelerate osteoporotic bone tissue regeneration. We have further suggested a method to insert these substances in ceramic scaffolds with high drug efficiency and performed a study of their simultaneous effect on the cellular activities of both osteoblasts and osteoclasts under in vitro conditions. Quercetin was selected as a representative

phytoestrogen and was incorporated homogeneously into CDHA scaffolds using our original room temperature 3D printing fabrication process. CDHA scaffolds with quercetin showed favourable mechanical properties as well the sustained release of drugs over long periods of time. Quercetin containing CDHA scaffolds showed superior osteoblast proliferation, differentiation, and mineralization compared with normal CDHA scaffolds and exhibited suppression of osteoclast proliferation and increased differentiation at the same time. The effect of quercetin on both cells was much higher than alendronate under the same dose amount. These outstanding results could further direct our attention to the development of more effective scaffolds for osteoporotic bone tissue regeneration. We expect that this simple and reproducible fabrication process will be adapted for the preparation of various ceramic scaffolds as multifunctional biomaterials to simultaneously promote healing and regeneration. More detailed in vivo studies of scaffold biological properties using osteoporosis models are currently in progress and will be the subject of future publications.

Acknowledgements

This work was supported by the Mid-Career Researcher Program through an NRF grant funded by The Korea Ministry of Education, Science, and Technology (MEST) (Number 2011-0017572). Authors greatly thank to Ms. Kim Seonyeon for her efforts and time to perform the real time-PCR study and to Dr. Seong (Korea Food Research Institute) for valuable discussion concerning phytochemicals.

References

1 B. Hohlweg-Majert, R. Schmelzeisen, B.M. Pfeiffer and E. Schneider, *Osteoporos. Int*., 2006, **17**,167–179.
2 E. Seeman, *J. Appl. Physiol*., 2003,**95**,2142–2151.
3 ACS cancer treatment information page. American Cancer Society website. Available at www.cancer.org /Treatment.
4 L. Kyllönen, M. D'Este, M. Alini and D. Eglin, *Acta Biomaterialia* , 2015,**11**,412–434.
5 J.A. Sterling and S.A. Guelcher, *Current osteoporosis reports,* 2014,**12**,48-54.
6 Y.Kinoshita and H. Maeda. The Scientific World Journal 2013;Article ID 863157, 21 pages http://dx.doi.org/10.1155/2013/863157.
7 P.J. Marie, *Bone,* 2006,**38**,10-14.
8 P.J. Marie, P. Ammann, G. Boivin and C. Rey, *Calcif. Tissue Int.,* 2001,**69**,121-129.
9 I.S. Kwun, Y.E. Cho, R. Lomeda, H.I. Shin, J.Y. Choi, Y.H. Kang and J.H. Beattie, *Bone,* 2010,**46**,732-741.
10 H. Zreiqat, C.R. Howlett, A. Zannettino, P. Evans, G. Schulze-Tanzil, C. Knabe, and M. Shakibaei, *J. Biomed. Mater. Res,* 2002,**62**,175-184.
11 M.P. Staiger, A.M. Pietak, J. Huadmai and G. Dias. *Biomaterials*, 2006,**27**,1728-1734.
12 E.M.Carlisle, *Science*, 1970,**167**,279-280.
13 H.D.Jung, S.W.Yook, C.M.Han, T.S.Jang, H.E.Kim, Y.H.Koh and Y.Estrin,J. Biomed. Mater. Res. B: Appl. Biomat.,2014,**102**,913-921.
14 S. Patntirapong, P. Habibovic and P.V. Hauschka, *Biomaterials,* 2009,**30**,548-555.
15 M. Fröhlich, W.L. Grayson, L.Q. Wan, D. Marolt, M. Drobnic and G. Vunjak-Novakovic, *Curr. Stem. Cell. Res. Ther.,* 2008,**3**,254–264.
16 R. Russell, N. Watts, F. Ebetino and M. Rogers, *Osteoporos. Int*., 2008,**19**,733–759.
17 J.S. Chen and P.N. Sambrook, *Nat. Rev. Endocrinol*., 2012,**8**,81–91.
18 J. Lee, M.M. Farag, E.K. Park, J. Lim and H.S. Yun, *Mat. Sci. and Engg. C,* 2014,**36**,252–260.
19 S. Bose and S. Tarafder, *Acta. Biomater.,* 2012,**8**,1401–1421.
20 M. Nakaya, H. Tachibana and K. Yamada, *Biochem. Pharmacology,* 2005,**71**,108-111.
21 M. Satue´, M.D.R. Arriero, M. Monjo and J.M. Ramis, *Biochem. Pharmacology,* 2013, **86**,1476–1486.
22 C.C. Araujo and L.L. Leon, *Mem. Inst. Oswaldo Cruz*,2001,**96**,723–728.
23 M. Yamaguchi, *J. Health Sci.,* 2002,**48**,209–222.
24 Q. Qu, M. Perala-Heape, A. Kapanen, J. Dahllund, J. Salo, H.K. Väänänen and P. Härkönen, *Bone*, 1998,**22**,201-209.
25 S. Kanno, S. Hirano and F. Kayama, *Toxicol.,* 2004,**196**,137-45.
26 M.M. Farag and H.S.Yun, *Materials Letters*, 2014,**132**,111–115.
27 H.S. Yun, S.E. Kim and Y.T. Hyeon, *Chem. Comm.,* 2007,2039-2141.
28 Online source: Available from Compositional guideline for Quercetin,dhy.:https://www.tga.gov.au/compositional-guideline-quercetin dihydrate+&cd=10&hl=en&ct=clnk&gl=jp
29 V. Viereck, H. Siggelkow, S. Tauber, D. Raddatz, N. Schutze and M. Hu¨fner, *J. Cell Biochem*., 2002,**186**,348-356.
30 H.S. Yun, S.H. Kim, D. Khang, J. Choi, H.H. Kim and M. Kang, *Int. J. of Nanomed.,* 2011,**6**,2521–2531.
31 D. Baksh, R. Yao, R.S. Tuan, *Stem Cells*, 2007,**25**,1384-1392.
32 J. Chen, H.S. Shapiro and J. Sodek, *J. Bone. Miner. Res.,* 1992,**7**,987-997.
33 G.C. Reilly, S. Radin, A.T. Chen and P. Ducheyne, *Biomaterials,* 2007,**28**,4091-4097.
34 P. Ballanti, S. Minisola, M.T. Pacitti, L. Scarnecchia, R. Rosso, G.F. Mazzuoli and E. Bonucci, *Osteoporosis Int.,* 1997,**7**,39-43.
35 J.C. Reichert, V.M.C. Quent, L.J. Burke, S.H. Stansfield, J.A. Clements and D.W. Hutmacher, *Biomaterials,* 2010,**31**,7928-7936.
36 S.Y. Sheu, C.C. Tsai, J.S. Sun, M.H. Chen, M.H. Liu and M.G. Sun, *Chin. Med. J. (Engl),* 2012,**125**,3646-3653.
37 R.W.K. Wong and A.B.M. Rabie, *The Open Orthopaedics J.,* 2008,**2**,27–32.
38 L.C. Chow, *Dental Mater. J.,* 2009,**28**,1-10.
39 Z. Jindong, T. Hai, G. Junchao, W. Bo, B. Li and W.B. Qiang, *Orthopedics*, 2010, **33**,11-16.
40 E. Boanini, P. Torricelli, M. Gazzano, R. Giardino and A. Bigia, *Biomaterials*, 2008,**29,**790–796.
41 A. Ehara, K. Ogata, S. Imazato, S. Ebisu, T. Nakano and Y. Umakoshi, *Biomaterials*, 2003,**24**,831–836.

Graphical abstract

Effect of direct loading of phytoestrogens into calcium phosphate scaffolds on osteoporotic bone tissue regeneration

G Tripathi, R. Naren and H.S. Yun*

Engineering Ceramics Division, Korea Institute of Materials Science (KIMS), 797 Changwondero, Changwon 641-831, Republic of Korea, yuni@kims.re.kr

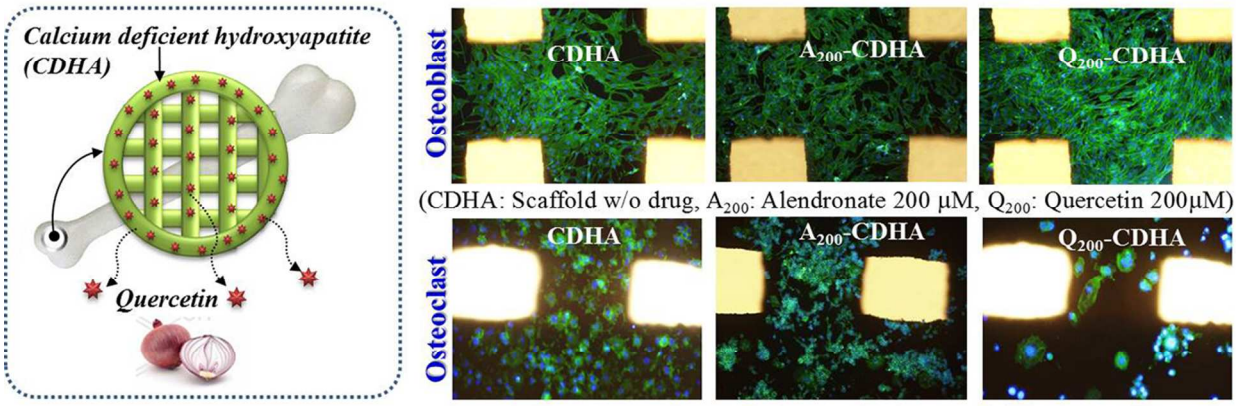

3D porous calcium deficient hydroxyapatite scaffolds with phytoestrogens were fabricated for osteoporotic bone tissue regeneration through a combination of 3D printing techniques and cement chemistry as a room temperature process.